A multifunctional integrated biomimetic spore nanoplatform for successively overcoming oral biological barriers

Qingling Song
Zhengzhou University
Junfei Yang
Zhengzhou University
Xiaocui Wu
Zhengzhou University
Jiannan Jiao
Zhengzhou University
Hongjuan Zhao
Zhengzhou University
Qianhua Feng
Zhengzhou University
Zhenzhong Zhang
Zhengzhou University
Yun Zhang
Zhengzhou University
Lei Wang (wanglei1@zzu.edu.cn)
Zhengzhou University

Research Article

Keywords: biomimetic spore, oral drug delivery, spore capsid, biological barrier

Posted Date: January 31st, 2023

DOI: https://doi.org/10.21203/rs.3.rs-2489677/v1

Version of Record: A version of this preprint was published at Journal of Nanobiotechnology on August 29th, 2023. See the published version at https://doi.org/10.1186/s12951-023-01995-z.

Abstract

The biological barriers have seriously restricted the efficacious responses of oral delivery system in diseases treatment. Utilizing a carrier based on the single construction means is hard to overcome these obstacles simultaneously because the complex gastrointestinal tract environment requires carrier to have different or even contradictory properties. Interestingly, spore capsid (SC) integrates many unique biological characteristics, such as high resistance, good stability etc. This fact offers a boundless source of inspiration for the construction of multi-functional oral nanoplatform based on SC without further modification. Herein, we develop a type of biomimetic spore nanoplatform (SC@DS NPs) to successively overcome oral biological barriers. Firstly, doxorubicin (DOX) and sorafenib (SOR) are self-assembled to form carrier-free nanoparticles (DS NPs). Subsequently, SC is effectively separated from probiotic spores and served as a functional vehicle for delivering DS NPs. As expect, SC@DS NPs can efficaciously pass through the rugged stomach environment after oral administration and further be transported to the intestine. Surprisingly, we find that SC@DS NPs exhibit a significant improvement in the aspects of mucus penetration and transepithelial transport, which is related to the protein species of SC. This study demonstrates that SC@DS NPs can efficiently overcome multiple biological barriers and improve the therapeutic effect.

1. Introduction

The gastrointestinal tract (GIT) is the principal region of most oral drugs delivery and therapeutic interventions [1]. Nevertheless, the multiple biological barriers of GIT have seriously restricted the efficacious responses of oral nanoparticles (NPs) in the intestinal diseases treatment [2, 3]. Considering the complexity of GIT environment, an optimal oral delivery system should be stable to prevent the premature drug release in the stomach [4]. Moreover, the delivery system also should efficiently address the critical obstacles including mucus and epithelial barriers, which requires the carrier to have different or even contradictory properties [5, 6]. For instance, the NPs surface that is close to electroneutrality charge is beneficial for escaping the mucus entrapment, but unfavorable to the epithelial cellular uptake, resulting in poor absorption and transepithelial transport [7]. At present, some substantial researches have constructed a variety of drug delivery carriers which could overcome these barriers by incorporating some specific functionalities and moieties mechanically [8–10]. However, the synthetic or modified carriers are complex and uncontrollable after administration, which might hinder the further absorption efficiency of NPs. Consequently, development of a simple and stable oral delivery nanoplatform for successively overcoming these aforementioned dilemmas is the focus of current research.

Recently, biomimetic strategy has emerged prevalent across a variety of fields such as drug delivery, biomaterial design and development, which has led to exciting advances [9, 11–14]. Interestingly, the unique protective mechanisms observed in nature, such as plant seed dormancy [15] and bacteria endospores [16], can protect their species from the interference of external environment, providing a blueprint for the development of “biomimetic nanoplatform”. Particularly, as the intrinsic structure of probiotic spores, the spore capsid (SC) integrates many unique biological characteristics, such as high

resistance, good stability etc.[17–19], which can be considered using in the construction of oral biomimetic spore system. However, SC would be disintegrated in the intestine during the spores germination and cannot be effectively utilized as the vehicle for delivering oral drugs [20]. As such, rational capitalizing SC based on a simple and efficient separation method is essential for the development of “biomimetic spore nanoplatform”. In this study, we found that SC containing various protein species which endowed it some unique biological activities such as “muco-inert” property and multi-receptor mediated endocytosis. These promising characteristics would provide clues to find alternative solutions for the oral drugs delivery.

In addition, combinational chemotherapy is still regarded as a primary strategy in the clinical treatment of colon cancer because it can overcome the drug resistance and heterogeneity issue of tumor cells [21–24]. As we previously reported, the chemotherapeutic (doxorubicin hydrochloride, DOX) and molecular targeted drugs (sorafenib, SOR) can be served as a synergistic therapeutic drug to enhance the therapeutic effect of colon cancer [25]. Although this synergistic strategy is promising, how to overcome the inherent limitations of these two free drugs, such as poor water solubility [26], rapid blood clearance [27] and low bioavailability [28], is still a big challenge. Considering that DOX with π-conjugated structure and a large number of hydroxyl groups can form stable hydrogen bonds with SOR. We speculated that DOX and SOR could be self-assembled to form carrier-free NPs (DOX/SOR NPs, DS NPs) through the interaction of hydrogen bonds and π-π stacking [29, 30]. Unfortunately, the DS NPs cannot resist to the harsh stomach environment and their use is usually limited by the side-effects that caused by systemic drug exposure.

Consequently, drawing inspiration by these unique characteristics of SC observed in probiotic spores, we firstly separated the total SC using an original method and determined its protein species by mass spectrometric analysis. And then based on SC, a new type of multifunctional integrated biomimetic spore nanoplatform (SC@DS NPs) was developed to successively overcome these aforementioned concerns in one-stop (Scheme 1). In this system, DOX and SOR were firstly prepared to be DS NPs by self-assembly and subsequently coated with SC that was separated from the probiotic spores. As expected, the results demonstrated that SC@DS NPs can successfully pass through the complex stomach environment, which was attributed to the protective delivery of SC. In addition, SC is rich in cysteine and with a large number of sulfhydryl groups, which can cleave the disulfide bonds between mucus glycoproteins, leading to good effect of evading the trap of mucus. Surprisingly, we found that SC@DS NPs exhibited a significant transepithelial transport efficiency, which was related to the proteins species of SC. We demonstrated that such biomimetic spore nanoplatform can successively overcome the mucosal diffusion barrier as well as the epithelial absorption barrier. Our work provided a simple and safe biomimetic nanoplatform that may help to guide the development of oral NPs delivery system.

2. Results And Discussion

2.1 The preparation and characterization of SC@DS NPs

As can be seen in the Scanning Electron Microscopy (SEM) and Transmission Electron Microscopy (TEM) images (Fig. 1a), spores with plump and integrity shape were separated successfully from probiotics. As shown in Fig. 1b, the morphology shrinkage of spores was observed after incubation with high concentration sodium chloride solution. Moreover, the TEM image showed the clear breaches in the spores where the red arrows point, which could cause the main content was released from spore. This phenomenon indicated that spore capsid (SC) was isolated successfully from the spores. Given the high resistance of SC to the harsh environment [17], we speculated that the SC could be served as a vehicle for delivering the nanoparticles (NPs) by oral administration. Furthermore, the strategy of combination of two drugs can be used to enhance the therapeutic effect [31–33]. Accordingly, as a proof of concept, the water-soluble doxorubicin hydrochloride (DOX) and hydrophobic sorafenib (SOR) were selected to form DS NPs by the nanoprecipitation method [30]. Surprisingly, as shown in Fig. 1c and Figure S1, the DS NPs were of good morphology, uniform particle size, and well dispersion. The UV absorption peak at 266 nm (red arrow) and 480 nm (black arrow) of DS NPs was consistent with the maximum absorption peak of free SOR and DOX, respectively, which further proved that the composition of DS NPs was DOX and SOR (Figure S2). Subsequently, as shown in Fig. 1d, compared with the DS NPs, the thick coating was observed on the surface of SC@DS NPs, which confirmed that SC@DS NPs were synthesized successfully. Moreover, the potent wrapping of SC onto the surface of DS NPs was further demonstrated by the slightly increased particle size and surface charge variations compared with the uncoated DS NPs (Figure S3 and Figure S4). And the protein composition of SC@DS NPs was similar to that of SC, indicating that SC coating process could not affect the surface composition of SC (Figure S5). With extension of the storage time at room temperature, the negligible changes of particle size and zeta potential illustrated the superior stability of SC@DS NPs (Figure S6).

Considering that spore coat is the key factor of spore resistance to the harsh acidic environment, we speculated that SC was relatively stable in stomach. In order to study whether SC could protect DS NPs from the extreme stomach condition, the DS NPs and SC@DS NPs were incubated in the simulated gastric fluid (SGF), respectively. After 2 h incubation, their morphologies were observed by TEM images. As shown in Fig. 1e, DS NPs were destroyed while SC@DS NPs could maintain the complete shape, which suggested that SC could be served as the protective vehicle. In addition, during the incubation in SGF, the drug release of DOX and SOR was also evaluated. As can be seen in Fig. 1f, the release amounts of DOX and SOR in DS NPs were close to 100%. On the contrary, the negligible release amount was detected in SC@DS NPs, which further testified the protective function of SC. Furthermore, the drug release properties and the morphology changes of DS NPs and SC@DS NPs were evaluated after both of the NPs were incubated in stimulated intestinal fluids (SIF) for 4 h, respectively. As shown in Fig. 1g, most DS NPs were broken (red arrow) and could not maintain a complete morphology. Although the SC@DS NPs could keep a good shape, there were still some slight damages because of the presence of intestinal specific enzymes, which could lead to a low drug release rate of about 30% in the SIF (Fig. 1h). And then, after the DS NPs and SC@DS NPs were pre-incubated in SIF for 4 h, they were transferred to the solution of pH 7.4 and pH 5.5 for another incubation time. As shown in Fig. 1i, the high release rate of DS NPs was detected in both pH 7.4 and pH 5.5. However, for the SC@DS NPs, there was almost no drug release after being

incubated in pH 7.4 for 20 h, while the sustained drug release was observed when they were transferred to the pH 5.5 solution. This result suggested that SC@DS NPs could achieve a sustained drug release in the tumor microenvironment.

Notably, mucus barrier could decrease the efficiency of the intestinal epithelial absorption of NPs [34]. We further analyzed the specific protein components of SC by LCMSMS (nanoLC-QE). As shown in Table S1, the SC contains amount of cysteine, which could lead to the high mucus penetration of SC. As we all know, mucus is composed of the complex biochemical compositions, which could adsorb a wide range of molecules and particles, including drugs, and other potentially harmful entities [35, 36]. As shown in Fig. 1j, a high aggregates rate was detected in the D/S treatment group, which was because the small molecule drugs could be trapped and quickly removed by intestinal mucus. Among these groups, SC@DS NPs showed a low aggregate rate with a percentage of 7.2% ± 4.7%, which could be interpreted as that SC containing amount of tyrosine could cleave the disulfide bonds between mucus glycoproteins, increasing the intestinal mucus penetration of DS NPs [37, 38]. Furthermore, the vertical distribution of NPs (red) on cell monolayer were observed by Confocal Laser Scanning Microscopy (CLSM) using Z-axial scanning (Figure S7). The fluorescence signals of DOX and DS NPs treatment groups exhibited a strong correlation with the mucus layer while very few signals were overlaid with the mucus for SC@DS NPs, indicating that a large proportion of SC@DS NPs could escape the trapping of mucus.

2.2 Uptake mechanism and transepithelial transport of SC@DS NPs

Efficient epithelium uptake and transepithelial transport play an essential role to the oral NPs delivery [39]. Firstly, the cytotoxicity of SC and SC@DS NPs was evaluated on Caco-2 cells, respectively. When the concentrations of SC and SC@DS NPs reached 500 μg/mL, the cell viability rate was about 95%, indicating that the drug carrier system has good biocompatibility and no obvious toxicity on Caco-2 cells (Figure S8). Notably, we found that the cell uptake rate on Caco-2 cells was significantly improved by SC@NPs compared with the other treated groups (Fig. 2a,b and Figure S9). This phenomenon is because SC has some target proteins which could bind to the receptors in epithelium. Intrigued by this promising result, we further investigated the endocytosis mechanism of SC@DS NPs. As shown in Fig. 2c, amiloride and M-β-CD were served as the non-specific inhibitors for macropinocytosis and pathway inhibitor of disruptor of lipid raft, respectively, which could significantly reduce the cellular uptake of the DS NPs treated group. Moreover, chlorpromazine and lovastatin were served as the inhibitors of clathrin-mediated endocytosis, and caveolae-mediated endocytosis pathways, respectively. Interestingly, SC@DS NPs displayed a marked inhibition effect of cellular uptake after being treated with chlorpromazine (11% reduction) and lovastatin (11.9% reduction), respectively. These results indicated that the cellular uptaken efficiency of SC@DS NPs was involved in the multiple cellular pathways such as lipid raft and caveolae-mediated uptake, clathrin-dependent endocytosis as well as macropinocytosis. As expected, this non-specificity of endocytosis pathway could contribute to the improvement of their cellular uptake efficiency.

Furthermore, we also studied the specific receptor-mediated endocytosis that related to the high uptake of SC@DS NPs. The previously studies claimed that the monocarboxylate transporter (MCT) was the main receptor in the transport of (short-chain fatty acid, SCFA), such as butyrate, lactate and propionate [40]. As shown in Fig. 2d, the cellular uptake of SC@DS NPs was evidently depressed by pravastatin (Pra) known as the inhibitor of MCT1. This result positively supported that MCT1 played a vital role for the endocytosis of SCFA-functionalized nanovehicles. Besides, the increased uptake rate in SC@DS NPs group might be associated with the extra activation of the other pathways. As reported, SC contains amount of tyrosine, which might enhanced the receptor-mediated endocytosis by the oligopeptide transporter (PePT1) [41]. The glycyl-sarcosine (Gly-Sar), as the inhibitor of the PePT1 receptor, could significantly decrease the uptake of SC@DS NPs. Without specific interaction with MCT1, SC@DS NPs still showed the high cellular uptake rate.

Subsequently, the *in vitro* transepithelial transport of different NPs was evaluated by the Caco-2 cell monolayers (Fig. 2e). To our surprise, as shown in Fig. 2f, the fluorescence of SC@DS NPs treatment group was embedded in the cell monolayer penetrating to the basal side of the monolayer. While the fluorescence of other groups was floating on the monolayer, and the penetrating phenomenon of these NPs was hardly observed. However, SC@DS NPs hardly achieved efficient transepithelial transport when the cell monolayers were incubated with the different pathway inhibitors, respectively. This result was interpreted by the fact that the transport efficiency of SC@DS NPs could be enhanced by the receptor mediated endocytosis. Additionally, the transepithelial electrical resistance (TEER) values of cell monolayer were nearly unchanged before and after the different treatments (Fig. 2g), which proved that the permeability of SC@DS NPs was caused by receptor-mediated transcellular transport rather than breakage of the integrity of cell monolayers. The amount of transcellular transport of SC@DS NPs was measured in basolateral chamber, exhibiting 2.6-fold and 2.9-fold ($P < 0.05$) higher than that of the group pre-treatment with Pra and Gly-sar, respectively (Fig. 2h). Meanwhile, the morphology of different NPs in basolateral chamber was detected by TEM. As shown in Fig. 2i, the edge of DS NPs was rough while the surface of SC@DS NPs with integrity was smooth, which indicated that SC@DS NPs had good stability when they were transported across the epithelium.

2.3 Evaluation of anti-tumor efficiency *in vitro*

The *in vitro* anti-tumor efficiency was investigated by the human colon tumor cell line SW620. As shown in Fig. 3a and Figure S10, there were no significant differences between DS NPs and SC@DS NPs treatment groups after 2 h and 4 h incubation, respectively. This result suggested that SC could only improve the intestinal epithelial transport efficiency due to the specific receptors, and it could not perform obvious cellular uptake in tumor cells. However, the cell uptake of DS NPs and SC@DS NPs was observably higher than that of DOX with the incubation time. Besides, the apoptosis level of different group in SW620 cells was also detected. As shown in Fig. 3b, there were more apoptotic cells in SC@DS NPs group with an apoptotic rate of 42.7 ± 3.0%, which was significantly higher than that of DS NPs treatment group (21.7 ± 2.2%) and D/S treatment group (21.5 ± 2.1%). This result was attributed to the fact that SC also could induce a mild apoptosis on tumor cells. The apoptosis level was further

determined by Western blotting analysis. As shown in Fig. 3c,d, a significant improvement in the apoptosis proteins such as caspase-9 and cleaved caspase-3 was observed after incubation with SC@DS NPs, indicating that SC@DS NPs could induce severe cell apoptosis. Moreover, the level of tumor cell apoptosis is also regulated by the antiapoptotic protein bcl-2 and the apoptotic protein bax [42]. The expression of bcl-2 and bax and the semi-quantitative analysis of bcl-2/bax ratio for each group were shown in Fig. 3e,f. For the SC@DS NPs treatment group, the bax/bcl-2 ratio was remarkably lower than that of the other groups, indicating that this preparation could enhance the process of cell apoptosis.

2.4 Intestinal absorption *in vivo*

The previous study claimed that the sulfhydryl groups of cysteine on the surface of spores could cleave the disulfide bond between mucin glycoproteins and improve the intestinal mucus penetration of NPs.[16] As shown in Fig. 4a and Figure S11, low fluorescence intensity was observed in the DOX-treated group, which indicated that DOX could not penetrate the mucus. For the DS NPs-treated group, though the marked fluorescence signal was detected, the intestinal epithelial cellular uptake exhibited a strong correlation with the mucus layer, indicating that a larger proportion of DS NPs was trapped within the mucus. This result was also demonstrated in the in vitro particles-mucin aggregation experiment. On the contrary, the higher fluorescence intensity was noticeably observed in the intestinal villi, while very few fluorescence signals were overlaid with the mucus. Moreover, as shown in Fig. 4b, the 3D images of the intestinal tissues with different treatment also proved that SC@DS NPs could dramatically avoid mucus trapping and improve the uptake efficiency of intestinal epithelial cells. This phenomenon can be interpreted as the protective functional of the SC.

For further investigating the in vivo intestinal absorption of different NPs, the mice were orally treated with free DOX, DS NPs and SC@DS NPs for 4 h, respectively. As shown in Fig. 4c, the weak red fluorescence signal was detected in the intestinal villi after the mice were treated with DS NPs, indicating the poor absorption of DS NPs. As expected, the strong fluorescence signal was obviously observed at both the epithelial cells and basolateral side of the epithelium in the SC@DS NPs treatment group. Interestingly, when the SC@DS NPs treated group was pre-incubated with Pra and Gly-sar, respectively, they exhibited a weak fluorescence signal in the epithelial cells. This result demonstrated that SC@DS NPs were efficiently absorbed at the epithelium and successfully transported into the lamina propria by the receptor-mediated endocytosis. Subsequently, the evaluation of in situ intestinal absorption and circulation was performed by the ex vivo ligated intestinal loop model. As shown in Fig. 4d, the amount of drug absorption of SC@DS NPs was 43.8% ± 3.5%, which was significantly higher than that of DS NPs with a drug absorption of 23.6% ± 3.9%. However, when the transcellular pathway was inhibited by Pra or Gly-sar, the intestinal epithelial absorption of SC@DS NPs was 13.2% ± 3.1% and 15.4% ± 2.8%, respectively. These results suggested that SC@DS NPs could increase the efficiency of transepithelial transport and absorption, which was the outstanding prerequisite to enhance the therapeutic effect.

Given the promising characteristics of SC@DS NPs, we further evaluated the oral relative bioavailability after administration with D/S, DS NPs, SC@DS NPs, SC@DS NPs + Pra and SC@DS NPs + Gly-sar,

respectively. The plasma concentration time curves and pharmacokinetic parameters were shown in Fig. 4e and Table S2. The C_{max} value of DS NPs was 1.24 ± 0.35 μg mL^{-1} at 1.5 h, which was lower than that of the other treatment groups. This result was mainly due to the poor stability of DS NPs when they passed through the harsh stomach conditions. Notably, the SC@DS NPs treated group achieved the highest relative bioavailability (F_{rel}), which was 5.6-fold higher than the values obtained by the DS NPs treatment. In addition, when the mice were pre-treated with the receptor inhibitors and followed by treatment with SC@DS NPs, their relative bioavailability was remarkably decreased. Taken together, SC@DS NPs with the superior mucus-penetrating and cellular uptake capabilities could be served as a valuable drug delivery system, improving the drugs bioavailability.

2.5 *In vivo* distribution and anti-tumor efficacy

For investigating the *in vivo* distribution of NPs, a near-infrared dye IR783 was employed to replace DOX to form the IR783 NPs self-assembly. As shown in Fig. 5a, the fluorescence signal notably accumulated into the stomach at 2 h for the free IR783 and IR783 NPs treatments, respectively. As time continued to extend, the rapid decrease of fluorescence distribution in vivo was clearly observed. By contrast, after the mice were treated with SC@IR783 NPs, the tumor site exhibited a strong fluorescence signal at 8 h and remained obvious fluorescence until 12 h, while the other treated groups displayed almost negligible fluorescence signal. This phenomenon of the NPs real-time distribution of the major organs and intestinal tissues could be interpreted as follows: i) SC could protect NPs from the harsh gastrointestinal tract environment; ii) SC could efficiently enhance the transepithelial transport ability of NPs by the multiple transport pathways, which could increase the amount of NPs that entered the bloodstream. These promising *in vivo* distribution characteristics of NPs might lead to a superior anti-tumor efficacy.

Subsequently, the in *vivo* tumor inhibition efficiency was investigated after treatment with saline, D/S, SC, DS NPs and SC@DS NPs for 14 days, respectively. As shown in Fig. 5b, the body weight gain of D/S and SC treated groups was slow because DOX had cardiotoxicity, while SC had only weak therapeutic effect. The body weight of the mice treated with SC@DS NPs was increased obviously, which suggested the good biocompatibility and treatment effect of SC@DS NPs. Moreover, the tumor volumes of each mouse were recorded to evaluate the treatment efficacy of different groups. As depicted in Fig. 5c and Figure S12, no obvious tumor inhibition was observed in saline and SC treatment groups. By comparing with the tumor volumes of D/S, DS NPs and SC@DS NPs treatment groups, the anti-tumor efficiency of SC-coated NPs on mice was better than that in free drugs and NPs group. Once the drug was prepared to the NPs and then functionalized with SC, the tumor inhibition efficacy was improved. These results showed that SC with good biosafety could be used as the vehicles for drug delivery and had an excellent protective effect on NPs, which can improve the stability of NPs in the complex GIT conditions and improve the anti-tumor effect.

Then the pathological features of small intestine and colon tissues were evaluated by the histology score changes according to the specific parameters (Table S3). As shown in Fig. 5d, the hematoxylin and eosin (H & E) assay suggested that D/S and DS NPs could induce the inflammatory reaction such as focal

lymphocytic infiltration; desquamation of epithelial cells and visible connective tissue hyperplasia in the lamina propri. However, there was no obvious inflammation was observed in the SC@DS NPs treatment group. Moreover, the groups based on the SC had almost negligible toxicity to the major organs (Figure S13), which indicated that the SC@DS NPs had a superior biosafety. As depicted in Fig. 5e, the closely arranged tumor tissues and complete morphology of tumor cells were clearly observed in the saline and SC treatment groups. On the contrary, the shrinkage of nuclei and the reduction of the tumor cells density were observed in the D/S and DS NPs groups. Interestingly, the most notable necrosis of tumor cells was detected in SC@DS NPs treatment, which proved the fact that SC could prevent the degradation of DS NPs from the GIT conditions and improve the in vivo anti- tumor efficacy. To further investigate the therapeutic effect of different treatment, we performed TUNEL assay to evaluate the tumor apoptosis characteristics. As expected, large amounts of substantial apoptosis/necrosis were significantly observed in SC@DS NPs group, which suggested that SC@DS NPs could inhibit the tumor development via inducing apoptosis pathway (Fig. 5f). These anti-tumor results were also proved by the expression of apoptotic or anti apoptotic proteins in the tumor tissues via immunofluorescence analysis (Fig. 5g and Figure S14-17). These above results suggested that SC@DS NPs have a superior anti-tumor effect.

3. Conclusion

In summary, learning from the biological characteristics of probiotic spores observed in nature, we rationally designed and developed a distinctive biomimetic spore nanoplatform (SC@DS NPs) to overcome both the mucosal diffusion barrier and the epithelial absorption barrier in one-stop. In this system, the SC integrated with multiple functions was served as a drug delivery vehicle. Compared with DS NPs, the SC@DS NPs retained the characteristic of probiotic spores, which could resist the extreme stomach acid environment after oral administration and subsequently deliver to the intestine successfully. Our study demonstrated that the NPs coated with SC were of lower mucin affinity and superior mucus penetration capability. This result was attributed to that the SC is rich in sulfhydryl groups that could cleave the disulfide bonds between mucus glycoproteins. We found that the intestinal epithelial absorption efficiency of SC@DS NPs was dramatically improved due to the SC containing some specific proteins. We demonstrated that such biomimetic spore nanoplatform can successively overcome the mucosal diffusion barrier and the epithelial absorption barrier only by coating SC on the surface of NPs.

Declarations

Competing interests

The authors declare no competing interests.

Acknowledgements

We gratefully acknowledge the National Natural Science Foundation of China (Nos. 81972907, 82171333, 82272847) and Modern Analysis and Computer Center of Zhengzhou University.

References

1. Lee Y, Deelman TE, Chen K, Lin DSY, Tavakkoli A, Karp JM: **Therapeutic luminal coating of the intestine.** *Nature Materials* 2018, **17:**834-+.

2. Duran-Lobato M, Niu Z, Alonso MJ: **Oral Delivery of Biologics for Precision Medicine.** *Advanced Materials* 2020, **32**.

3. Ahadian S, Finbloom JA, Mofidfar M, Diltemiz SE, Nasrollahi F, Davoodi E, Hosseini V, Mylonaki I, Sangabathuni S, Montazerian H, et al: **Micro and nanoscale technologies in oral drug delivery.** *Advanced Drug Delivery Reviews* 2020, **157:**37-62.

4. Song Q, Jia J, Niu X, Zheng C, Zhao H, Sun L, Zhang H, Wang L, Zhang Z, Zhang Y: **An oral drug delivery system with programmed drug release and imaging properties for orthotopic colon cancer therapy.** *Nanoscale* 2019, **11:**15958-15970.

5. Lundquist P, Artursson P: **Oral absorption of peptides and nanoparticles across the human intestine: Opportunities, limitations and studies in human tissues.** *Advanced Drug Delivery Reviews* 2016, **106:**256-276.

6. Fan W, Xia D, Zhu Q, Li X, He S, Zhu C, Guo S, Hovgaard L, Yang M, Gan Y: **Functional nanoparticles exploit the bile acid pathway to overcome multiple barriers of the intestinal epithelium for oral insulin delivery.** *Biomaterials* 2018, **151:**13-23.

7. Cui Y, Shan W, Liu M, Wu L, Huang Y: **A strategy for developing effective orally-delivered nanoparticles through modulation of the surface "hydrophilicity/hydrophobicity balance".** *Journal of Materials Chemistry B* 2017, **5:**1302-1314.

8. Blanco E, Shen H, Ferrari M: **Principles of nanoparticle design for overcoming biological barriers to drug delivery.** *Nature Biotechnology* 2015, **33:**941-951.

9. Wu J, Zheng Y, Liu M, Shan W, Zhang Z, Huang Y: **Biomimetic Viruslike and Charge Reversible Nanoparticles to Sequentially Overcome Mucus and Epithelial Barriers for Oral Insulin Delivery.** *Acs Applied Materials & Interfaces* 2018, **10:**9916-9928.

10. Garcia-Diaz M, Birch D, Wan F, Nielsen HM: **The role of mucus as an invisible cloak to transepithelial drug delivery by nanoparticles.** *Advanced Drug Delivery Reviews* 2018, **124:**107-124.

11. Yang X, Zhou T, Zwang TJ, Hong G, Zhao Y, Viveros RD, Fu T-M, Gao T, Lieber CM: **Bioinspired neuron-like electronics.** *Nature Materials* 2019, **18:**510-+.

12. Chen Z, Wang Z, Gu Z: **Bioinspired and Biomimetic Nanomedicines.** *Accounts of Chemical Research* 2019, **52:**1255-1264.

13. Maslanka Figueroa S, Fleischmann D, Goepferich A: **Biomedical nanoparticle design: What we can learn from viruses.** *Journal of controlled release : official journal of the Controlled Release Society* 2021, **329:**552-569.

14. Zhu X, Wu J, Shan W, Zhou Z, Liu M, Huang Y: **Sub-50 nm Nanoparticles with Biomimetic Surfaces to Sequentially Overcome the Mucosal Diffusion Barrier and the Epithelial Absorption Barrier.** *Advanced Functional Materials* 2016, **26:**2728-2738.

15. Chong LSH, Zhang J, Bhat KS, Yong D, Song J: **Bioinspired cell-in-shell systems in biomedical engineering and beyond: Comparative overview and prospects.** *Biomaterials* 2021, **266**.

16. Yin L, Meng Z, Zhang Y, Hu K, Chen W, Han K, Wu BY, You R, Li CH, Jin Y, Guan YQ: **Bacillus spore-based oral carriers loading curcumin for the therapy of colon cancer.** *Journal of Controlled Release* 2018, **271:**31-44.

17. Wu IL, Narayan K, Castaing JP, Tian F, Subramaniam S, Ramamurthi KS: **A versatile nano display platform from bacterial spore coat proteins.** *Nature Communications* 2015, **6:**6777.

18. Clair G, Esbelin J, Mallea S, Bornard I, Carlin F: **The spore coat is essential for Bacillus subtilis spore resistance to pulsed light, and pulsed light treatment eliminates some spore coat proteins.** *International Journal of Food Microbiology* 2020, **323**.

19. McKenney PT, Driks A, Eichenberger P: **The Bacillus subtilis endospore: assembly and functions of the multilayered coat.** *Nature Reviews Microbiology* 2013, **11:**33-44.

20. Setlow P: **Germination of Spores of Bacillus Species: What We Know and Do Not Know.** *Journal of Bacteriology* 2014, **196:**1297-1305.

21. Kaluzki I, Hailemariam-Jahn T, Doll M, Kaufmann R, Balermpas P, Zoeller N, Kippenberger S, Meissner M: **Dimethylfumarate Inhibits Colorectal Carcinoma Cell Proliferation: Evidence for Cell Cycle Arrest, Apoptosis and Autophagy.** *Cells* 2019, **8**.

22. Qin S-Y, Cheng Y-J, Lei Q, Zhang A-Q, Zhang X-Z: **Combinational strategy for high-performance cancer chemotherapy.** *Biomaterials* 2018, **171:**178-197.

23. Yu W, Shevtsov M, Chen X, Gao H: **Advances in aggregatable nanoparticles for tumor-targeted drug delivery.** *Chinese Chemical Letters* 2020, **31:**1366-1374.

24. Zhang H, Dong S, Li Z, Feng X, Xu W, Tulinao CMS, Jiang Y, Ding J: **Biointerface engineering nanoplatforms for cancer-targeted drug delivery.** *Asian Journal of Pharmaceutical Sciences* 2020, **15:**397-415.

25. Song Q, Zheng C, Jia J, Zhao H, Feng Q, Zhang H, Wang L, Zhang Z, Zhang Y: **A Probiotic Spore-Based Oral Autonomous Nanoparticles Generator for Cancer Therapy.** *Adv Mater* 2019, **31:**e1903793.

26. Wei X, Liu L, Li X, Wang Y, Guo X, Zhao J, Zhou S: **Selectively targeting tumor-associated macrophages and tumor cells with polymeric micelles for enhanced cancer chemo-immunotherapy.** *Journal of Controlled Release* 2019, **313:**42-53.

27. Zhao T, Zhou H, Lei L, Guo C, Yang Q, Gong T, Sun X, Song X, Gong T, Zhang Z: **A new tandem peptide modified liposomal doxorubicin for tumor "ecological therapy".** *Nanoscale* 2020, **12:**3359-3369.

28. Zeng S, Ou H, Gao Z, Zhang J, Li C, Liu Q, Ding D: **HCPT-peptide prodrug with tumor microenvironment -responsive morphology transformable characteristic for boosted bladder tumor chemotherapy.** *Journal of controlled release : official journal of the Controlled Release Society* 2020, **330:**715-725.

29. Wu H, Wang C, Sun J, Sun L, Wan J, Wang S, Gu D, Yu C, Yang C, He J, et al: **Self-Assembled and Self-Monitored Sorafenib/Indocyanine Green Nanodrug with Synergistic Antitumor Activity Mediated by Hyperthermia and Reactive Oxygen Species-Induced Apoptosis.** *Acs Applied Materials & Interfaces* 2019, **11:**43996-44006.

30. Shamay Y, Shah J, Isik M, Mizrachi A, Leibold J, Tschaharganeh DF, Roxbury D, Budhathoki-Uprety J, Nawaly K, Sugarman JL, et al: **Quantitative self-assembly prediction yields targeted nanomedicines.** *Nature Materials* 2018, **17:**361-+.

31. Li Y, Lin J, Ma J, Song L, Lin H, Tang B, Chen D, Su G, Ye S, Zhu X, et al: **Methotrexate-Camptothecin Prodrug Nanoassemblies as a Versatile Nanoplatform for Biomodal Imaging-Guided Self-Active Targeted and Synergistic Chemotherapy.** *Acs Applied Materials & Interfaces* 2017, **9:**34650-34665.

32. Zhang A, Hai L, Wang T, Cheng H, Li M, He X, Wang K: **NIR-triggered drug delivery system based on phospholipid coated ordered mesoporous carbon for synergistic chemo-photothermal therapy of cancer cells.** *Chinese Chemical Letters* 2020, **31:**3158-3162.

33. Wei L, Chen J, Ding J: **Sequentially stimuli-responsive anticancer nanomedicines.** *Nanomedicine* 2021, **16:**261-264.

34. Xu Q, Ensign LM, Boylan NJ, Schoen A, Gong X, Yang J-C, Lamb NW, Cai S, Yu T, Freire E, Hanes J: **Impact of Surface Polyethylene Glycol (PEG) Density on Biodegradable Nanoparticle Transport in Mucus ex Vivo and Distribution in Vivo.** *Acs Nano* 2015, **9:**9217-9227.

35. Murgia X, Loretz B, Hartwig O, Hittinger M, Lehr C-M: **The role of mucus on drug transport and its potential to affect therapeutic outcomes.** *Advanced Drug Delivery Reviews* 2018, **124:**82-97.

36. Bansil R, Turner BS: **The biology of mucus: Composition, synthesis and organization.** *Advanced Drug Delivery Reviews* 2018, **124:**3-15.

37. Menzel C, Bernkop-Schnuerch A: **Enzyme decorated drug carriers: Targeted swords to cleave and overcome the mucus barrier.** *Advanced Drug Delivery Reviews* 2018, **124:**164-174.

38. Ren T, Wang Q, Xu Y, Cong L, Gou J, Tao X, Zhang Y, He H, Yin T, Zhang H, et al: **Enhanced oral absorption and anticancer efficacy of cabazitaxel by overcoming intestinal mucus and epithelium barriers using surface polyethylene oxide (PEO) decorated positively charged polymer-lipid hybrid nanoparticles.** *Journal of Controlled Release* 2018, **269:**423-438.

39. Yang D, Liu D, Deng H, Zhang J, Qin M, Yuan L, Zou X, Shao B, Li H, Dai W, et al: **Transferrin Functionization Elevates Transcytosis of Nanogranules across Epithelium by Triggering Polarity-Associated Transport Flow and Positive Cellular Feedback Loop.** *ACS Nano* 2019, **13:**5058-5076.

40. Wu L, Liu M, Shan W, Zhu X, Li L, Zhang Z, Huang Y: **Bioinspired butyrate-functionalized nanovehicles for targeted oral delivery of biomacromolecular drugs.** *Journal of Controlled Release* 2017, **262:**273-283.

41. Bemena LD, Mukama O, Neiman AM, Li Z, Gao X-D, Nakanishi H: **In vitro reconstitution of the yeast spore wall dityrosine layer discloses the mechanism of its assembly.** *Journal of Biological Chemistry* 2017, **292:**15880-15891.

42. Wang L, Hu Y, Hao Y, Li L, Zheng C, Zhao H, Niu M, Yin Y, Zhang Z, Zhang Y: **Tumor-targeting core-shell structured nanoparticles for drug procedural controlled release and cancer sonodynamic combined therapy.** *Journal of Controlled Release* 2018, **286:**74-84.

Schemes

Scheme 1 is available in the supplementary files section.

Figures

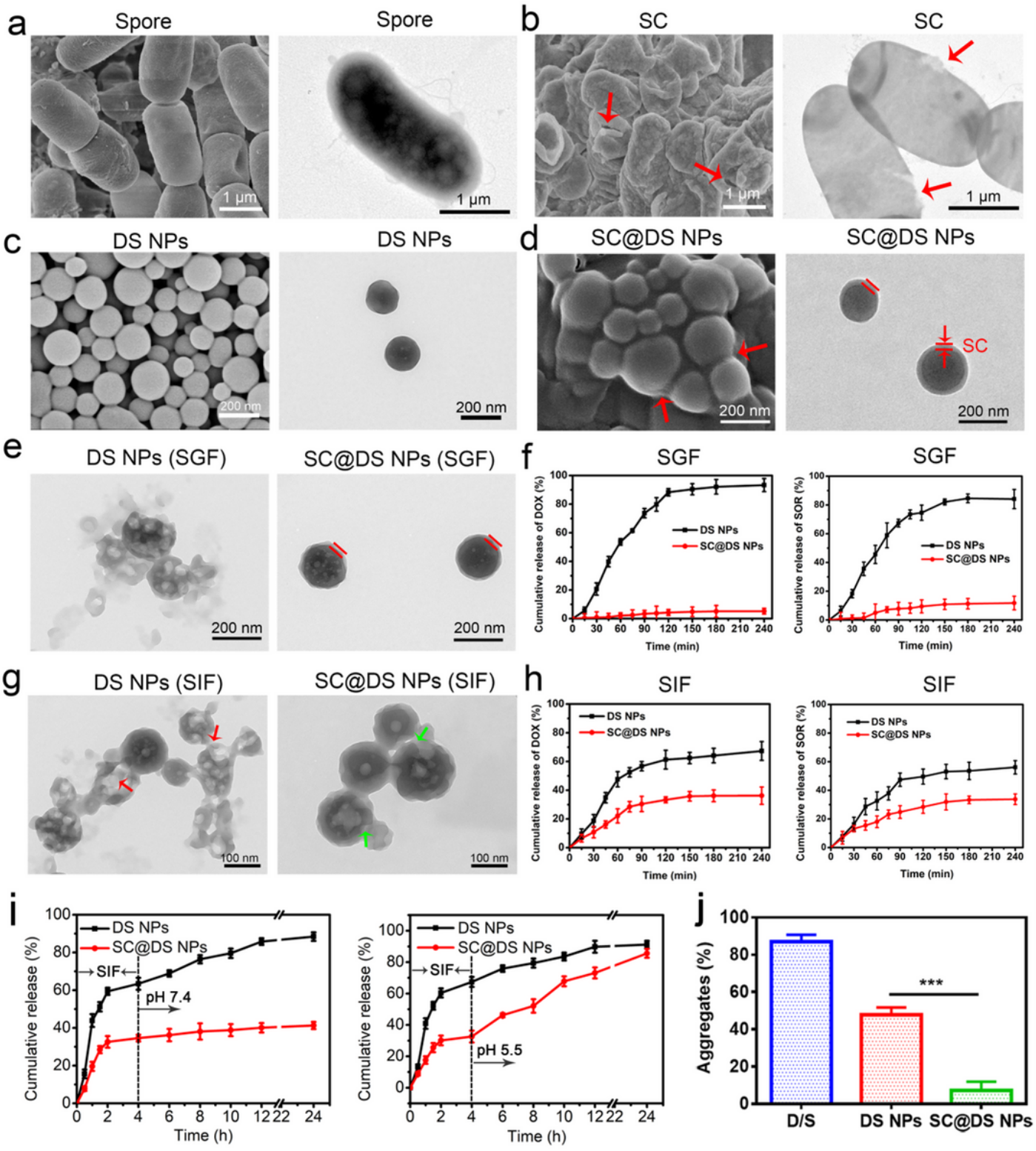

Figure 1

Preparation and characterization. SEM and TEM images of a) spores and b) SC, respectively. The SEM and TEM images of c) DS NPs and d) SC@DS NPs, respectively. e) The morphologies of DS NPs and SC@DS NPs were investigated after 2 h incubation in SGF. f) The cumulative DOX and SOR release of DS NPs and SC@DS NPs in SGF. g) The morphology changes of DS NPs and SC@DS NPs after 4 h incubation in simulated gastric fluid (SGF). h) The cumulative release amount of SOR and DOX in DS

NPs and SC@DS NPs groups after being incubated in SGF for 4 h. i) The release behavior of drugs from DS NPs and SC@DS NPs after being incubated in a buffer with gradually varying pH for over 24 h. j) The percentage of particles-mucin aggregation formed in simulated mucus solution for different preparations at 37°C.

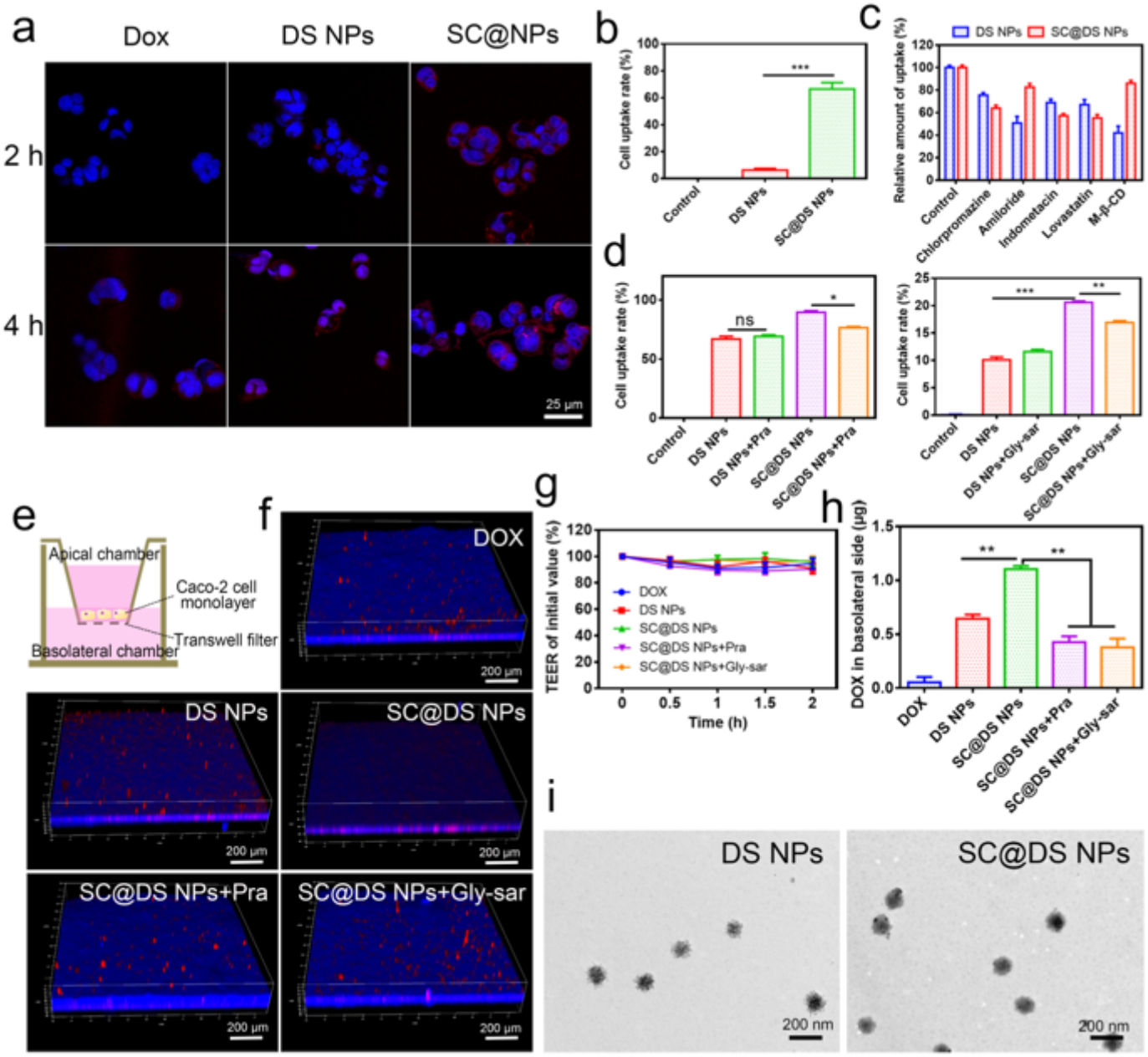

Figure 2

Studies of uptake mechanism and transepithelial transport. a) Cell uptake of free DOX, DS NPs and SC@DS NPs at 2 h and 4 h incubation, respectively. b) Flow cytometry analysis of the cell uptake of DS NPs and SC@DS NPs after 4 h incubation. c) The measurement of relative uptake on Caco-2 cells after being incubated with the different endocytosis inhibitors. d) The influences of Pra and Gly-sar on the cellular uptake of DS NPs and SC@DS NPs, respectively. e) Establishment of Caco-2 cell monolayer models. f) The CLSM images of different NPs on Caco-2 cell monolayers from apical to basolateral side.

g) TEER values of Caco-2 cell monolayers before and after different incubations. h) The amount of transepithelial transport of different groups in the basolateral chamber. i) The TEM images of DS NPs and SC@DS NPs in the basolateral chamber.

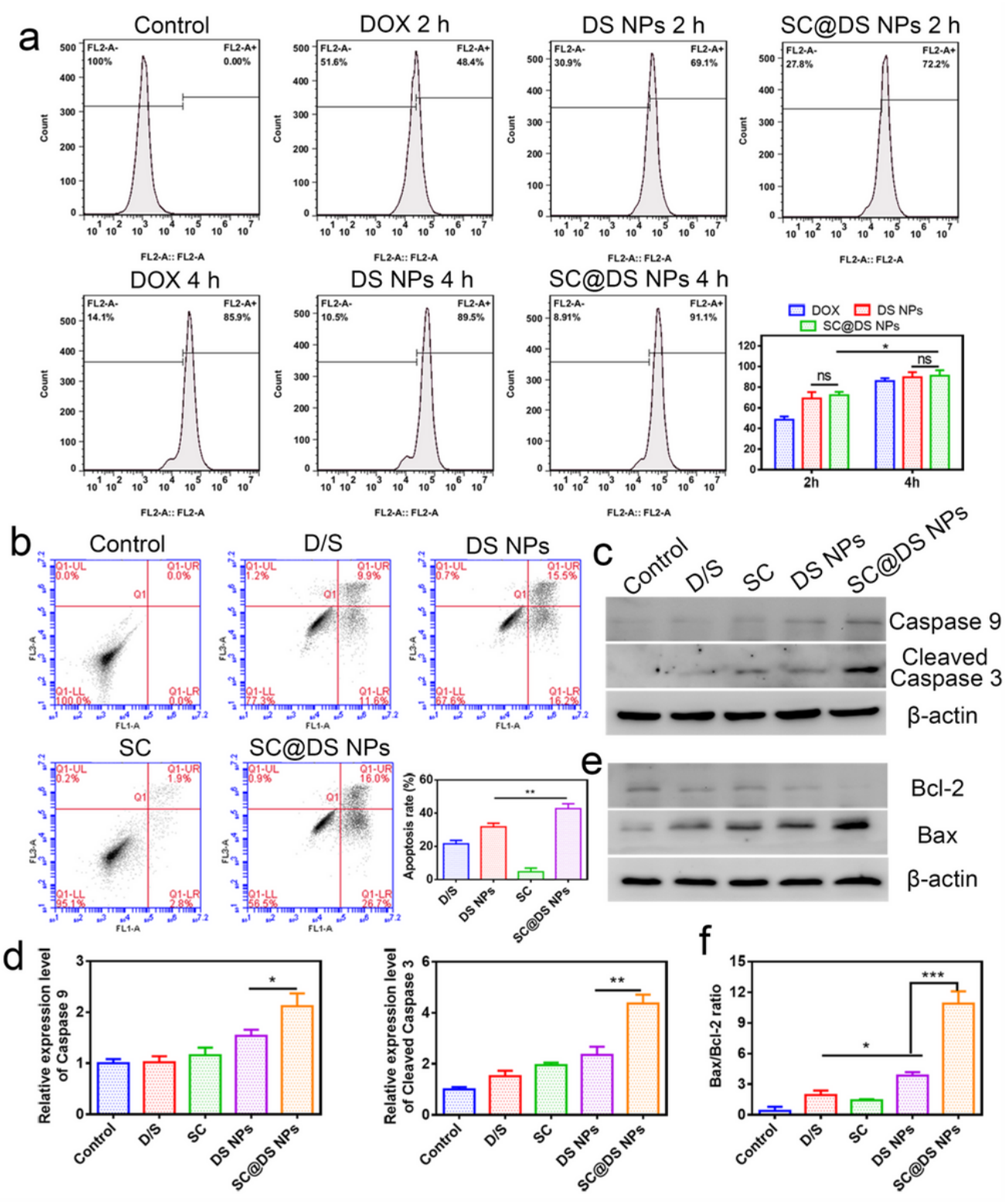

Figure 3

Cellular uptake and apoptosis analysis in SW620 tumor cells. a) Quantitative determination of cell uptake amounts for free DOX, DS NPs and SC@DS NPs at 2 h and 4 h incubation, respectively. b) Apoptosis level of SW620 cells after being treated with D/S, DS NPs, SC and SC@DS NPs, respectively. c) The casepase-9 and cleaved-caspase-3 protein levels of SW620 cells and d) semi-quantitative analysis of different groups. e) The expression level of bcl-2 and bax and the bcl-2/bax ratio analysis.

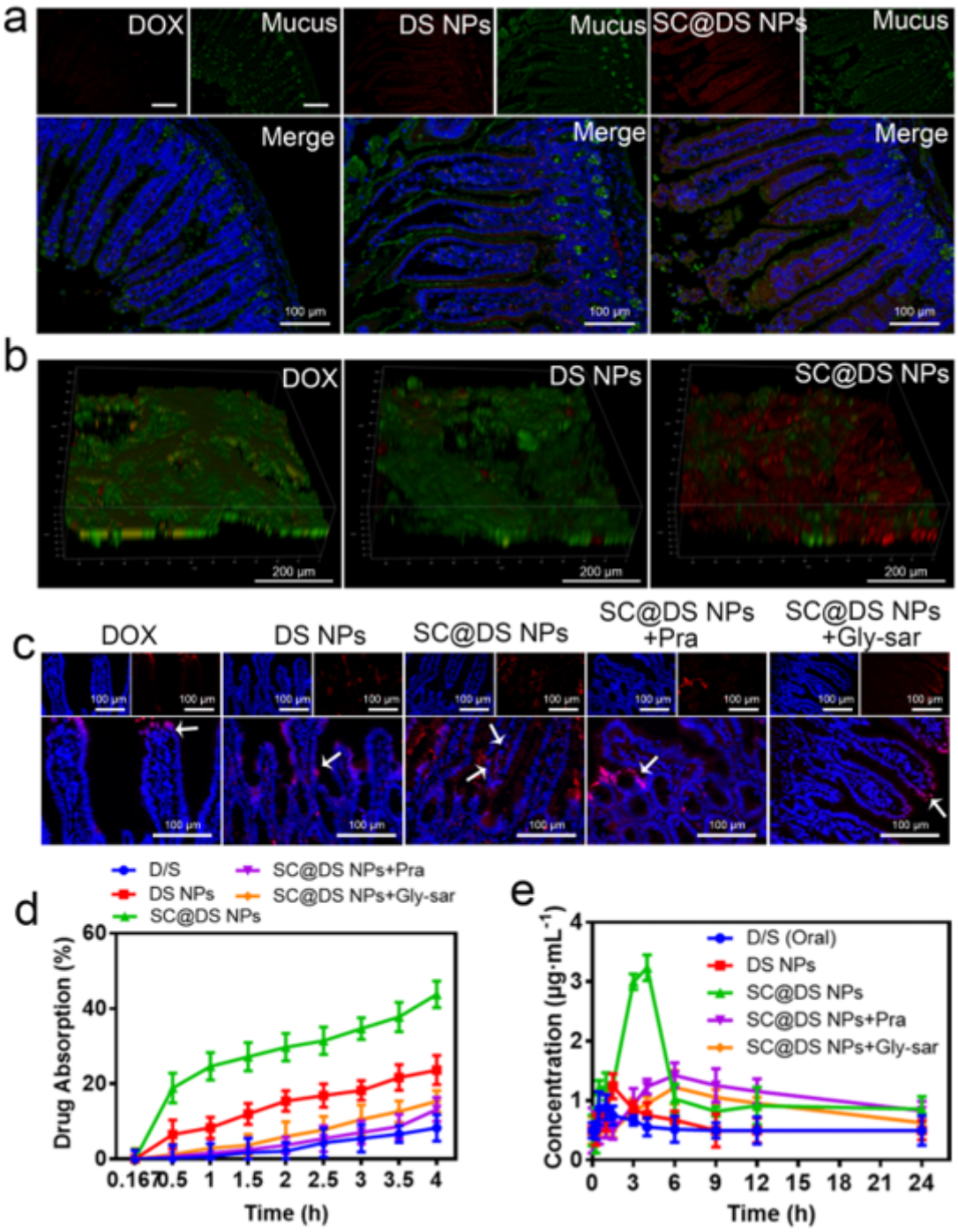

Figure 4

Evaluation of intestinal absorption and pharmacokinetic parameters. a) The mucus penetration effect of different NPs. b) The typical 3D CLSM images of the different NPs distribution in mucus. c)

Representative fluorescence images of intestine after the mice were treated with free DOX, DS NPs, SC@DS NPs, SC@DS NPs + Pra and SC@DS NPs + Gly-sar by gavage, respectively. d) Evaluation of the intestinal absorption of different groups by the in situ intestinal circulation and absorption model. e) Drug concentration in plasma after oral administration with different groups at a dose equivalent to 30 mg kg^{-1} of DOX.

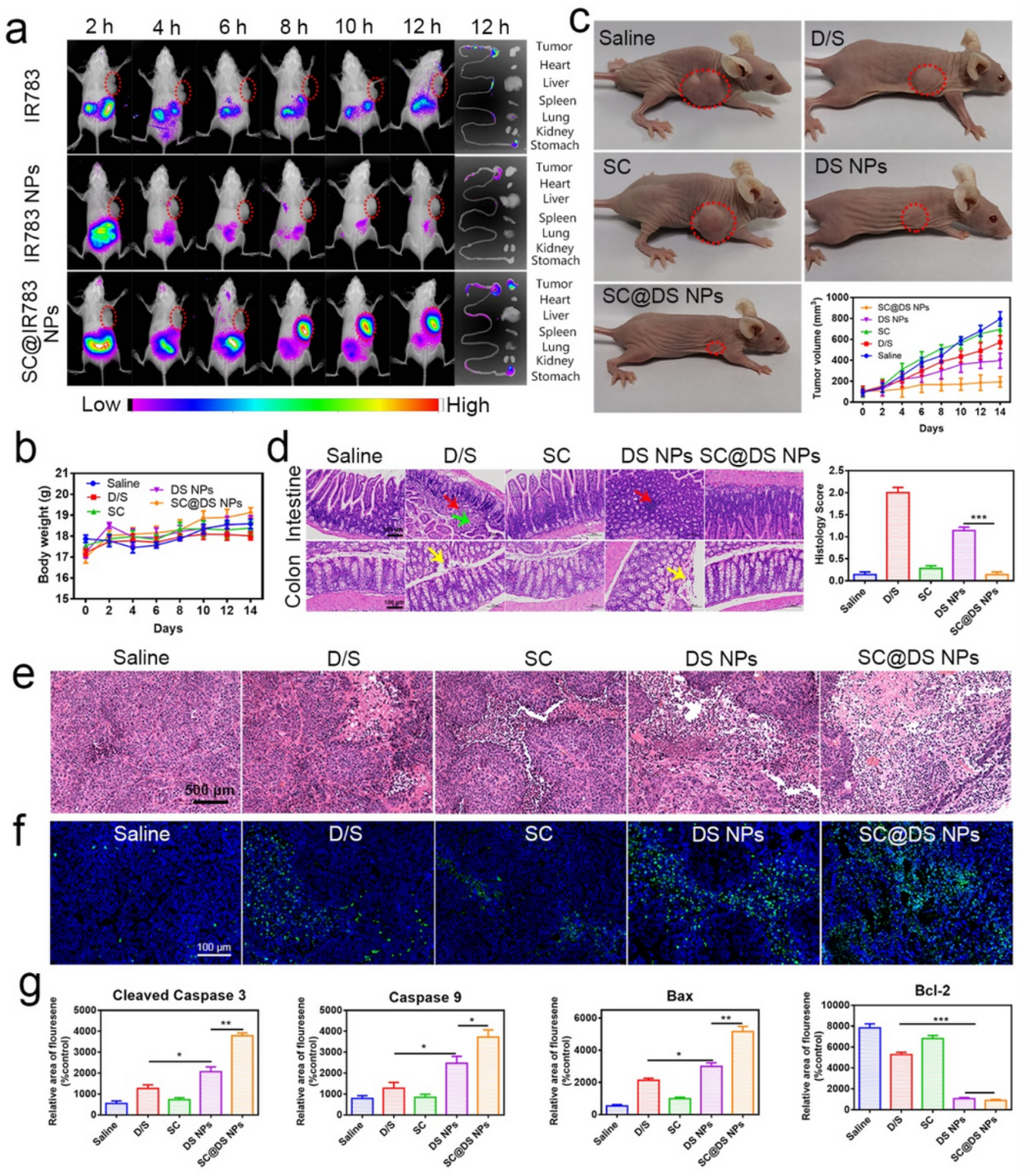

Figure 5

The *in vivo* distribution and treatment efficacy of different NPs. a) *In vivo* imaging of SW620 tumor-bearing mice at preset time points after oral administration with different NPs. b) The body weight changes of different treatments. c) Representative pictures of mice after different treatments. d) Representative H&E images of intestinal and colorectal tissues and histology score after different treatments (Red arrow: focal lymphocytic infiltration; Yellow arrow: desquamation of epithelial cells, Green arrow: visible connective tissue hyperplasia in the lamina propria), Scale bar = 100 μm. e) H&E staining of tumor tissues from different treatments (Scale bar = 500 μm). f) TUNEL staining of tumor tissues at the end of each treatments (Scale bar = 100 μm). g) Quantitative analysis of apoptosis and anti-apoptosis related proteins including cleaved caspase-3, caspase-9, bax, and bcl-2 in different treatments (mean ± SD, n = 6, $*P < 0.05$, $**P < 0.01$, $***P < 0.001$). The different formulations were orally administered to rats at a dose equivalent to 30 mg kg^{-1} of DOX and 5 mg kg^{-1} of SOR, respectively. Significant differences were assessed using two-way analysis of variance (ANOVA) with multiple comparisons or using the t-test for comparison of two groups.

Supplementary Files

This is a list of supplementary files associated with this preprint. Click to download.

- Supportinginformation2023118.docx
- Scheme.docx